

Review

Calcium Imaging Perspectives in Plants

Chidananda Nagamangala Kanchiswamy ^{1,*}, Mickael Malnoy ¹, Andrea Occhipinti ² and Massimo E. Maffei ²

¹ Research and Innovation Centre Genomics and Biology of Fruit Crop Department, Fondazione Edmund Mach (FEM), Istituto Agrario San Michele (IASMA), Via Mach 1, 38010 San Michele all'Adige (TN), Italy; E-Mail: mickael.malnoy@fmach.it

² Department of Life Sciences and Systems Biology, Innovation Centre, University of Turin, Via Quarello 15/A, 10135 Turin, Italy; E-Mails: andrea.occhipinti@unito.it (A.O.); massimo.maffei@unito.it (M.E.M.)

* Author to whom correspondence should be addressed; E-Mail: chidananda.nagamangala@fmach.it; Tel.: +39-461-615-133; Fax: +39-461-650-956.

Received: 23 December 2013; in revised form: 18 February 2014 / Accepted: 20 February 2014 / Published: 4 March 2014

Abstract: The calcium ion (Ca^{2+}) is a versatile intracellular messenger. It provides dynamic regulation of a vast array of gene transcriptions, protein kinases, transcription factors and other complex downstream signaling cascades. For the past six decades, intracellular Ca^{2+} concentration has been significantly studied and still many studies are under way. Our understanding of Ca^{2+} signaling and the corresponding physiological phenomenon is growing exponentially. Here we focus on the improvements made in the development of probes used for Ca^{2+} imaging and expanding the application of Ca^{2+} imaging in plant science research.

Keywords: calcium; transcription factors; calcium probes; imaging

1. Introduction

Knowledge of Ca^{2+} signaling and its corresponding physiological phenomenon from prokaryotes to eukaryotes and from tissues to whole organisms has grown significantly. For the past six decades, calcium signaling has been a focus of study with a level of investigation higher than that of any other signaling molecule. In plants, numerous endogenous stimuli and stress signals of both biotic and

abiotic nature lead to transient variation in intracellular Ca^{2+} concentration, which in turn activate respective downstream signaling cascades [1–6]. Studying the role of intracellular Ca^{2+} requires the ability to monitor the dynamics of its concentration in plant cells with both spatial and temporal accuracy [7–9].

In plants, the concentration of cytosolic Ca^{2+} ($[\text{Ca}^{2+}]_{\text{cyt}}$) is maintained in the nano molar range (100–200 nM) while in many organelles it may reach micro molar to mili molar concentrations [10,11]. Vacuole and apoplast shows mili molar Ca^{2+} concentration [12]. The use of new generation cameleon and aequorin (AEQ) has led to the discovery of Ca^{2+} dynamics at micor molar level in ER lumen and at nM level in mitochondria and peroxisomes [13–19]. In plant cells, the spatial and temporal dynamic changes of $[\text{Ca}^{2+}]_{\text{cyt}}$ induced by various stimuli determine the final functional outcome [9,20]. Therefore, in plant cells, determining changes of $[\text{Ca}^{2+}]_{\text{cyt}}$ is largely dependent on the development of methodologies that can be used to accurately measure $[\text{Ca}^{2+}]_{\text{cyt}}$ [21,22].

Here, we describe the development of various Ca^{2+} probes from the past six decades and the improvements that have been developed in this field. We also discuss the limitations of each probe and important points to consider while planning ideal Ca^{2+} imaging experiments in plant science.

2. Measuring $[\text{Ca}^{2+}]_{\text{cyt}}$ in Living Plant Cells

Confocal microscopy is an optical sectioning method used to reduce the image blur that is caused by inclusion of light from outside the plane-of-focus in a cross-section of a thick sample. In confocal microscopy, the path of out-of-focus light is physically blocked before detection [23]. As a comparatively non-destructive imaging technique, confocal laser scanning microscopy (CLSM) has a number of distinct advantages over alternative imaging modalities; primarily CLSM facilitates the *in situ* characterization of the 3D architecture of tissue microstructure [24]. Several papers addressed the benefits that CLSM affords during analysis of the spatial properties of intracellular $[\text{Ca}^{2+}]$ signals [20]. However, it is generally difficult to measure $[\text{Ca}^{2+}]$ in a non-invasive method and without artifacts. It is also particularly tricky to measure $[\text{Ca}^{2+}]$ in a physiologically relevant context, which allows the comparison of results obtained in the laboratory with the physiological status of plants in the field. CLSM makes extensive use of Ca^{2+} probes. However, not only CLSM can offer the possibility to couple the use of Ca^{2+} probes with *in vivo* microscopy analyses. Wide-field fluorescent microscopy has been used for both dyes and genetically encoded probes. $[\text{Ca}^{2+}]_{\text{cyt}}$ was determined using the dye Fura-2 by either fluorescence ratio with a Cairn micro photometer [25] or fluorescence ratio imaging with a GenIV-intensified Pentamax-512 charge-coupled device camera [26]. By using high-resolution deconvolution microscopy, Allen and co-workers [27] assessed the cytoplasmic localization and auto fluorescence at both emission wavelengths of cameleon, YC2.1. Recently, Costa and co-workers used Selective Plane Illumination Microscopy (SPIM) which is an imaging technique particularly suited for long term *in vivo* analysis of transparent specimens, able to visualize small organs or entire organisms, at cellular and eventually even subcellular resolution. SPIM was successfully used in calcium imaging based on Förster Resonance Energy Transfer (FRET) in *Arabidopsis* seedlings expressing the cytosolic (NES-YC3.6) or nuclear (NLS-YC3.6) localized Cameleon YC3.6 [28].

3. Origin and Evolution of Synthetic Ca²⁺ Indicators

In the early 1960s to 1970s, many synthetic indicators such as murexide, azo dyes, and chlortetracycline were used as Ca²⁺ indicators [29]. Among the limitations of these synthetic indicators are a low sensitivity (azo dyes), the impossibility to be used to measure Ca²⁺ in living cells (murexide) and a low accuracy (chlortetracycline) [30]. The first fluorescent Ca²⁺ probe ideal for intracellular Ca²⁺ measurement was synthesized by Roger Tsien in the late 1980s [29]. Later on, a range of synthetic dyes was developed with desirable sensitivity, selectivity and responsiveness to measure Ca²⁺ in living plant cells [8,21]. Moreover, the evolution of AEQ [31,32], green fluorescent protein (GFP) [33] and FRET [34,35] based Ca²⁺ fluorescent imaging became more popular because of their user friendly Ca²⁺ measurement methods; however, Ca²⁺ fluorescent dyes have the advantages of being applicable to plants not suitable for transformation.

4. Measurement of Ca²⁺ Using Non-Ratiometric Dyes or Single Wavelength Probes

Ca²⁺ probes (also referred as sensors or reporters) are small molecules that show desirable features of sensitivity, selectivity and responsiveness to Ca²⁺. These probes form selective complexes with Ca²⁺ ions, which enable measurement of the differences in free and bound [Ca²⁺] using absorbance and emission light [36–38]. Most of the Ca²⁺ imaging probes interact with Ca²⁺ through carboxylic acid groups. This interaction causes variation in indicator properties such as fluorescent intensity and its excitation. [Ca²⁺] is not measured directly; rather the indicator monitors the amount of free and complexed probe. The concentration of free Ca²⁺ is then measured based on effective dissociation constant (K_d) measured *in vitro* of the probe for Ca²⁺ in the specific environment.

[Ca²⁺]_{cyt} is measured based on relative increase in fluorescence intensity of single wavelength. Non-ratiometric dyes such as fluo, rhod and Calcium Green-1 are used for measuring [Ca²⁺]_{cyt} in plants, among them Calcium Green-11 is well-known and most commonly used in plant systems. The single excitation spectrum allows for simple instrumentation. A simple formula is used to calculate the absolute Ca²⁺ concentration in live plant cells.

$$[\text{Ca}^{2+}] = K_d \times \frac{F - F_{\min}}{F_{\max} - F}$$

where K_d is the dissociation constant for Ca²⁺ for the fluorescent dye which is measured *in vitro*; F stands for fluorescence measured; F_{\min} is the fluorescence of the probe in the absence of Ca²⁺ and F_{\max} is the fluorescence of the probe at saturation point [39]. Calibration of absolute Ca²⁺ in *in vitro* samples are much easier using this method compared to ratiometric dyes but *in vivo* measurement in plant cells is a challenging task compared to animal cells. In an animal cell, it is easier to use mild detergent to permeabilize the entry of the Ca²⁺ dye through the plasma membrane, but in plants, the cell wall forms a major barrier. In plant and animal cells, limitations of this method are: corrections cannot be made for photobleaching, unequal dye loading, movements of dye within the cell and changes in optical density of the cell which affects the fluorescent intensity and accurate measurement of Ca²⁺. Moreover, these dyes are sensitive to pH, ionic strength and the surrounding protein environment, which alters their properties [7,8,21]. In order to overcome these limitations, it is recommended to simultaneously collect information on Ca²⁺-dependent fluorescence and probe concentration [30].

Other limitations such as optical artifacts could be overcome by using ratiometric dyes. These dyes offer robust approaches for *in vivo* quantitative measurement of Ca^{2+} based on fluorescence changes.

5. Measurement of Ca^{2+} Using Ratiometric Dyes

The excitation spectrum of ratiometric dyes Fura-2 and Indo-1, varies according to the free Ca^{2+} concentration. The Ca^{2+} concentration is measured as the ratio between two fluorescence intensity values that are taken at two wavelengths; *i.e.*, increasing wavelength λ_1 and decreasing wavelength λ_2 . The absolute $[\text{Ca}^{2+}]$ can be calculated using the following formula:

$$[\text{Ca}^{2+}] = K_d \times \frac{R - R_{\min}}{R_{\max} - R} \times \frac{F_{\max}^{\lambda_1}}{F_{\min}^{\lambda_1}}$$

where K_d is the dissociation constant, which is measured *in vitro*; R is the fluorescence ratio at both wavelengths $F^{\lambda_2}/F^{\lambda_1}$; R_{\min} is the minimum ratio value (it can be at minimum or maximum calcium concentration, depending on the wavelength used in the denominator); R_{\max} is the maximum ratio value; $F_{\max}^{\lambda_1}/F_{\min}^{\lambda_1}$ is a scaling factor, also known as β (F^{λ_1} is the fluorescence used in the denominator at its maximum and minimum value).

Ratiometric dyes can be corrected for unequal dye loading, photobleaching and focal plane shift, between two cells that have the same $[\text{Ca}^{2+}]_{\text{cyt}}$. Therefore using ratios avoids many of the problems related to absolute fluorescence values. On the other hand, acquisition and data manipulation is more complex due to the use of fluorescence ratios. Not all microscopes are suitable for these measurements (changing excitation/emission wavelength at suitable rates is required) and many ratiometric indicators require the use of UV excitation, which is an expensive option for confocal laser scanning microscopy.

It is important to note that dyes are available at different ranges of K_d values and spectral properties, that make them suitable for commonly used lasers [40].

6. Techniques of Loading Ca^{2+} -Sensing Dyes into Plant Cells

Most of the Ca^{2+} interacting dyes used for Ca^{2+} measurement have highly charged groups, hence they are relatively membrane impermeable; therefore, loading probes in living plant cells is a challenging task [21]. Many loading techniques have been successfully adopted to breach the plasma membrane such as microinjection, electroporation, patch clamp pipette and biolistic delivery [41–44]. Acid and ester methods are also adopted to introduce Ca^{2+} dyes; the acid method is based on pH changes. Acid loading for a 1–2 h incubation causes a drop in pH to 4.5 and protonates the dye to breach the plasma membrane in a relatively uncharged form [45,46]. Samples are incubated for 1–2 h at low pH, which might cause adverse effects on plant cells and tissues. In case of ester loading, acetoxymethyl esters are generally used for intracellular cellular cleavage by cellular esterases to deliver the Ca^{2+} dye into cytosol [30]. Ester loading causes significant hydrolysis in the plant cell wall but loading and incubation at low temperature may limit this problem [47]. Another major problem of Ca^{2+} interacting dyes is their compartmentalization in cellular organelles, mainly in the vacuole [45,48]. Compartmentalization means that the indicator is trapped within cellular organelles and not homogeneously distributed throughout the plant cell [22].

Table 1. Cont.

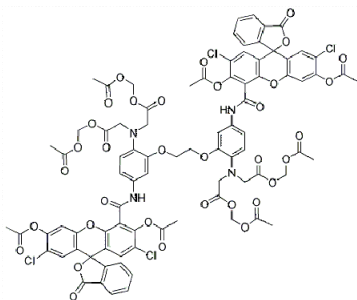
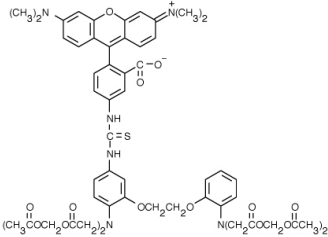
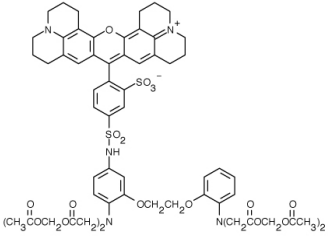
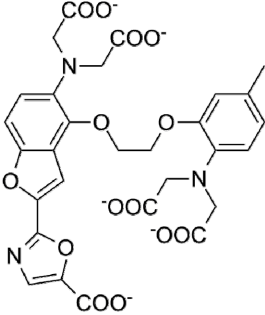
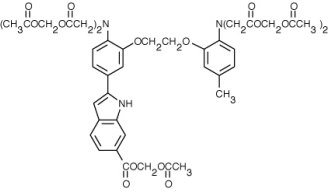
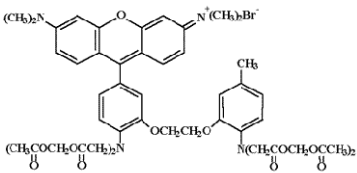
Ca ²⁺ indicator	Chemical structure	Properties	References
CALCIUM GREEN™-2		It has two fluorescent reporter groups, which are believed to quench one another in the absence of calcium, that undergo a much larger increase in fluorescence emission upon calcium binding than does Calcium Green™-1. Its lower affinity for calcium makes it particularly suited to measuring relatively high spikes of calcium, up to 25 μM.	[58]
CALCIUM ORANGE™		These are spectrally similar to tetramethylrhodamine and Texas Red. The long-wavelength spectral characteristics of these indicators allow them to be used in combination with fluorescein and ultraviolet excitable dyes.	[37,44,50,59]
CALCIUM CRIMSON™			
INDO-1		These are “dual-emission” and “dual-excitation” types of calcium dyes, respectively. To utilize either of these indicators, however, appropriate modifications of standard CLSM need to be made, such as a high-power argon-ion laser is required to obtain ultraviolet (UV) excitation, and compensatory changes along the optical path must be incorporated to deal with the lens aberrations and reduced signal throughputs that are associated with UV illuminations. At low concentrations of the indicator, use of the 340/380 nm excitation ratio for Fura-2 or the 405/485 nm emission ratio for Indo-1 allows accurate measurements of the intracellular Ca ²⁺ concentration. Measurements of Indo-1 and Fura-2 fluorescence can usually be made over a period of an hour without significant loss of fluorescence resulting from either leakage or bleaching. In addition, Fura-2 and Indo-1 are bright enough to permit measurements at intracellular concentrations of dye unlikely to cause significant Ca ²⁺ buffering or damping of Ca ²⁺ transients.	[11,46,60]
FURA-2			

Table 1. Cont.

Ca ²⁺ indicator	Chemical structure	Properties	References
RHODAMINE-BASED INDICATORS.		<p>Rhod-2 has fluorescence excitation and emission maxima at 552 and 581 nm, respectively. Variants with longer-wave length excitation and emission (X-Rhod-1) and lower Ca²⁺-binding affinity (Rhod-5N, Rhod-FF, <i>etc.</i>) have been developed (<i>i.e.</i>, at Molecular Probes). Rhod-2 is used as a selective indicator for mitochondrial Ca²⁺ in most eukaryotic cells.</p>	[11]

7. Protein Based Ca²⁺ Indicators

7.1. Aequorin-Based Ca²⁺ Indicators

Aequorin (AEQ) photoprotein has been extensively used in the Ca²⁺ signaling field for almost 40 years. AEQ is a Ca²⁺-binding photoprotein composed of an apoprotein (apoaquorin), which has an approximate molecular weight of 22 kDa and a prosthetic group, a luciferin molecule, coelenterazine (Mr 432). In the presence of molecular oxygen, the functional holoprotein, aequorin, reconstitutes spontaneously. The protein contains three EF-hand Ca²⁺-binding sites. When these sites are occupied by Ca²⁺, aequorin undergoes a conformational change and behaves as an oxygenase that converts coelenterazine into excited coelenteramide, which is released together with carbon dioxide. When the excited coelenteramide relax to its ground state, blue light ($\lambda = 469$ nm) is emitted [20]. This emitted light can be easily detected with a luminometer and correlates with the particular [Ca²⁺]. Identification of Ca²⁺ sensitive AEQ from *Aequorea victoria* offers enormous advantage to carry out bioluminescence research. This protein was carefully extracted and purified from jelly fish to prevent the contact with Ca²⁺ as this would cause chemiluminescence, there by rendering the protein unsuitable for Ca²⁺ measurements [61]. These proteins have been extensively engineered to obtain several luminescent probes with different biological parameters [62–64]. With the advanced genetic engineering and cloning strategies, it is possible to specifically localize them within the cell by including specific targeting amino acid sequences [41].

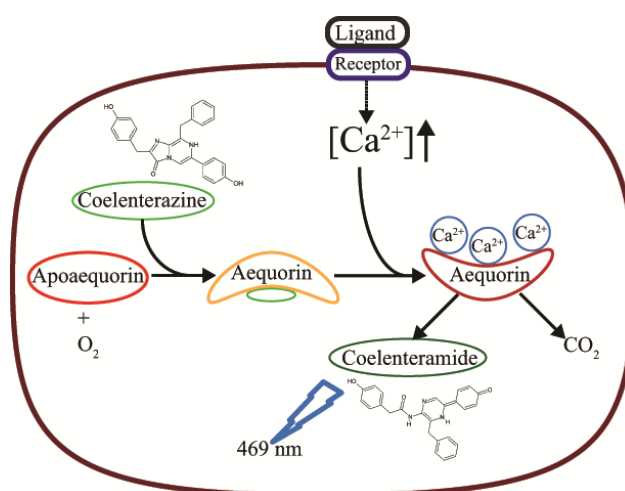
In the last two decades the study of Ca²⁺ dynamics in living cells has been enhanced by a significant improvement of genetically encoded protein based indicators [62]. AEQ allows their endogenous production in cell system as diverse as bacteria, yeast, fungi, plants and mammalian cells.

The new generation of bioluminescent probes coupled with Ca²⁺ sensitive AEQ allows real time measurement of Ca²⁺ changes [65,66]. Recently, AEQ based luminescent recording system has been developed to monitor spatiotemporal Ca²⁺ dynamics to various stimuli in Arabidopsis plants [63].

A major advantage of AEQ is that it can be selectively targeted to subcellular compartments by insertion of signal sequences unlike chemical compound dyes (excluding rhod-2, which is largely retained in the mitochondrial matrix). Use of recombinant AEQ facilitated the understanding of Ca²⁺ signaling interplay between different cellular compartments [67–72]. AEQ became less popular because of its small inherent signal; although the amount of signal emitted by the cell population is quite adequate to measure Ca²⁺ concentration, the signal from single cell is very low. Adequate

quantity of signal is needed to overcome background noise at the expense of space and time resolutions. One of the limitations of AEQ use is that it usually overestimates the real response of cells, especially when cell suspensions are used instead of whole tissues. For instance, when comparing Fluo-3AM responses in Lima bean leaf tissues and AEQ signals in soybean cell suspensions, the upper level of estimated level of Ca^{2+} in soybean cell culture responsiveness to H_2O_2 corresponds to the lower level in both mechanically damaged and herbivore wounded Lima bean leaves. This situation reflects the higher sensitivity of cell suspensions cultures compared to plant tissues, and should be considered for further comparisons when AEQ is used to evaluate activities of molecules involved in signaling processes [73]. However, not only suspension cell cultures expressing AEQ have been used, but also seedlings or leaf discs. For example, Matri and co-workers [74] used GAL4 transactivation of AEQ to analyze $[\text{Ca}^{2+}]_{\text{cyt}}$ signaling in specific cell types, including those of the leaves. Therefore, AEQ can offer tissue specificity if placed under control of tissue-specific promoters.

Figure 1. Mechanism of light emission by AEQ upon Ca^{2+} -binding. The apoprotein (Apoaequorin) binds the prosthetic group Coelenterazine, a luciferine molecule. In the presence of oxygen, the holoprotein AEQ reconstitutes spontaneously. The EF-hand Ca^{2+} -binding site on AEQ binds free Ca^{2+} , which cause conformational changes in the aequorin. Through oxygenase activity, aequorin converts Coelenterazine into excited Coelenteramide and carbon dioxide. Coelenteramide relaxes to ground state by releasing blue light (469 nm).



In AEQ assays the emitted light is calibrated into Ca^{2+} concentrations by a method based on the calibration curve of Allen and coworkers [75]:

$$[\text{Ca}^{2+}] = \frac{\left(\frac{L_0}{L_{\max}}\right)^{\frac{1}{3}} + \left[KTR \times \left(\frac{L_0}{L_{\max}}\right)^{\frac{1}{3}} - 1 \right]}{KR - \left[KR \times \left(\frac{L_0}{L_{\max}}\right)^{\frac{1}{3}} \right]}$$

where L_0 is the luminescence intensity per second and L_{\max} is the total amount of luminescence present in the entire sample over the course of the experiment. $[\text{Ca}^{2+}]$ is the calculated Ca^{2+} concentration,

KR is the dissociation constant for the first Ca^{2+} ion to bind, and KTR is the binding constant of the second Ca^{2+} ion to bind to AEQ [20]. Figure 1 shows the principle of the AEQ reaction.

7.2. GFP-Based Ca^{2+} Indicators

GFP based Ca^{2+} sensors are immediate alternatives to synthetic dyes and AEQ described above. In 1997 the first GFP based recombinant Ca^{2+} probe was developed [33,76]. Even though there are many indicators, a limited number of those have been used in plants [77]. Currently there are three main types of this Ca^{2+} sensor: cameleons, camgaroos and pericams [61,78,79]. All these sensors were based on calmodulin (CaM) as a regulator, which changes its conformation and alters fluorescence properties upon binding to Ca^{2+} . The cameleon probe has been extensively used in plant science research as compared to camgaroos and pericams [7,8,21,27]. These probes are chimeric proteins designed on the property called change of FRET, first synthesized by Tsien and co-workers [79,80]. FRET occurs between two different colored GFP mutants, with spectral overlap of the donor emission spectrum and the acceptor absorption spectrum. In the probe, the two GFP mutants are linked together by CaM and CaM binding peptide [80]. Binding of Ca^{2+} to the Ca^{2+} -responsive elements alters the efficiency of FRET. Like AEQ, several generations of FRET-based Ca^{2+} were synthesized with different biological parameters, sensitivity and efficiency; among them yellow cameleon (YC2.1) is the most popular for their use under different physiological conditions [80,81]. The YC2.1 version of cameleon has been widely used in plants for measurements of Ca^{2+} fluxes in guard cells, Nod factor responses, rhizobium and fungal colonization in the roots [27,82–85]. Later on various modified version of cameleon sensors were used to dissect subcellular Ca^{2+} dynamics; for example, D3cpv cameleon sensor for peroxisome Ca^{2+} flux and YC4.6 for pollen tube endoplasmic reticulum Ca^{2+} dynamics [17,19]. Two recent works report the use of D3cpv for mitochondrial Ca^{2+} analysis and D4ER for ER Ca^{2+} analysis [14,15]. Considering their importance in measuring Ca^{2+} dynamics at subcellular levels, efforts were made to develop a new generation of YC2.1 with significantly increased FRET signal to provide efficient Ca^{2+} measurements while reducing signal to noise ratio, this modified version was named YC3.6 [61,79,86]. This new generation with high-resolution signal has been widely used in plants for spatiotemporal imaging of cytoplasmic Ca^{2+} fluxes [87,88]. Recently YC3.6 has been successfully used to measure the cytosolic Ca^{2+} upon mechanical damage and herbivory in Arabidopsis leaves [89]. A wide range of YC sensors were successfully employed in plant science to analyze the spatiotemporal Ca^{2+} flux in different cell types such as guard cells, root, root hairs, pollen tube and different subcellular compartments [13,17,90–92]. Successes of the cameleon-based sensors are limited by CaM binding peptide as part of the sensing mechanism. Endogenous CaM could interfere with the sensor and could possibly change FRET signal.

Leaves of plants expressing FRET-based Ca^{2+} sensor YC3.6 can be ratio-imaged by CLSM. The YC3.6 Ca^{2+} sensor is usually excited at 458-nm wavelength by using an argon laser. The cyan fluorescent protein (CFP) and FRET-dependent Venus emission are assayed using a krypton/argon laser at 458 nm with a 473–505 and 526–536 nm emission filters. *In situ* calibration is performed through raising Ca^{2+} to saturating levels for YC3.6. Cells are usually permeabilized to allow a massive free diffusion of calcium inside the cell to get the R_{\max} . EGTA and EDTA can trap the free calcium released from the cells. Therefore, the maximum FRET/CFP ratio is obtained by treatment with

1 molar CaCl₂ in response to mechanical perturbation. The minimum FRET/CFP ratio is recorded by treatment with 1 molar Tris 100 mM EDTA and 50 mM EGTA solution. [Ca²⁺]_{cyt} variations are then calculated according to the equation:

$$[Ca^{2+}] = \frac{K_d \times (R - R_{min})}{(R_{max} - R)^{1/n}}$$

where *R* represents the FRET/CFP ratio measured during the experiment, *n* the Hill coefficient for YC3.6 (usually = 1), while *K_d* values are assessed for a given concentration of Ca²⁺ [88]. Figure 2 illustrates the determination of [Ca²⁺]_{cyt} variations using a cameleon probe.

Figure 2. (A) Fluorescence emission spectrum of cameleon YC 3.6 FRET-based Ca²⁺ sensor. The increase of Ca²⁺ concentration increase the emission from YFP (FRET-acceptor); (B) In absence of free Ca²⁺, the donor protein (CFP) releases the absorbed energy as fluorescence at 480 nm. In the presence of Ca²⁺, the calmodulin and M13 domains bind the free Ca²⁺. The conformational change of chimeric protein allows FRET to occur between the donor fluorescent protein CFP and the acceptor fluorescent protein YFP with light emission at 530 nm.

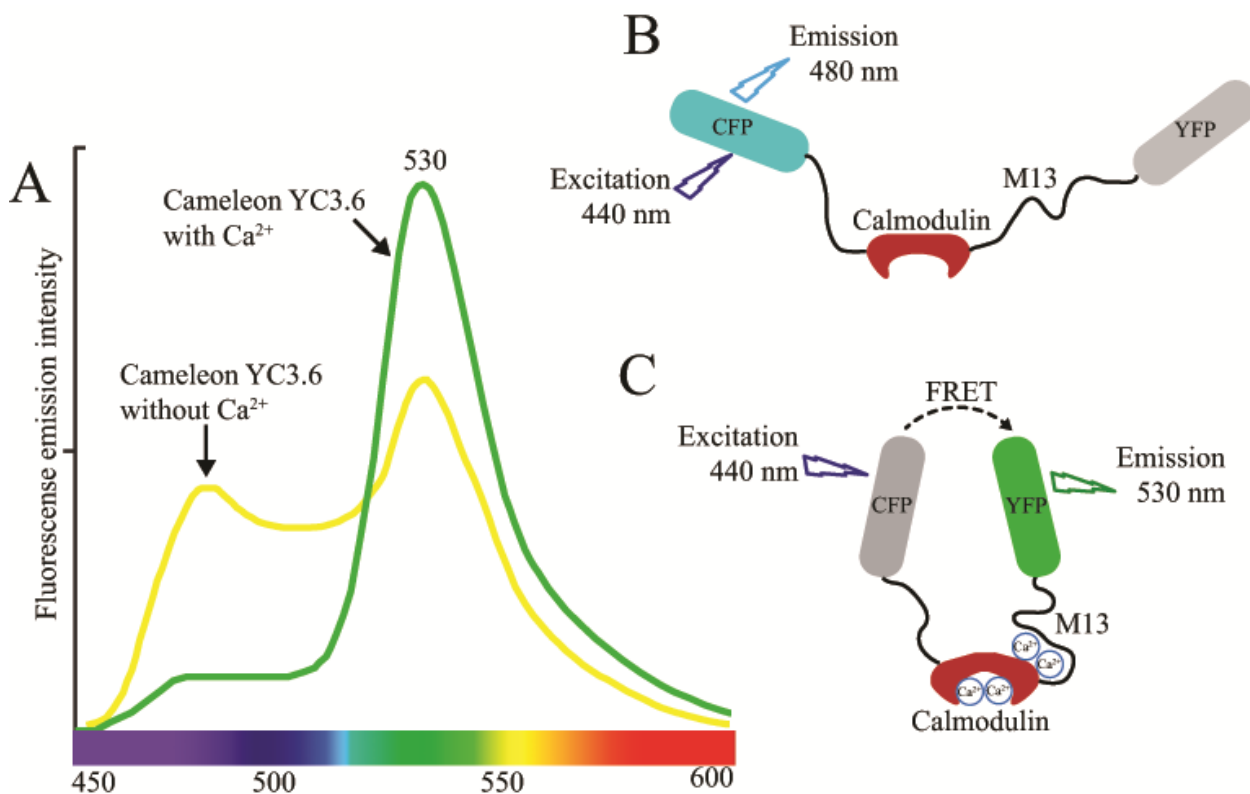


Table 2 lists some of the most used GFP-based Ca^{2+} indicators in plant sciences.

Table 2. Main GFP-based Ca^{2+} indicators used in plant science.

Cameleon family	Suitability	Stimulus/response	References
YC2.1	Suitable to use under various physiological condition because of their lower sensitivity to pH.	Ca^{2+} fluxes in <i>Arabidopsis</i> guard cells, Ca^{2+} elicitation in NOD factor of <i>medicago trunculata</i> , Ca^{2+} role in plant interaction with symbiotic bacteria (rhizobium) and fungal (mycorrhizal) root colonization.	[27,33,82–85,93–96]
Nucleoplasmin-YC2.1	Suitable for nuclear matrix localization study	Sieberer and colleague showed that Ca^{2+} spiking localized to nuclear matrix in the root hairs in response to external nodulation factors.	[97]
D3cpv	Suitable for studying peroxisomal Ca^{2+} dynamics	Costa and colleagues showed peroxisomal Ca^{2+} dynamics under stress signaling.	[17]
YC4.6	Suitable for studying endoplasmic reticulum Ca^{2+} dynamics	Iwano and colleagues showed pollen tube endoplasmic reticulum Ca^{2+} dynamics	[19]
YC3.6	Substitution of acceptor yellow fluorescent protein yielded five fold increased signal sensitivity, which allowed imaging of both temporal and dynamic signaling of cytosolic Ca^{2+} fluxes.	Used to study Ca^{2+} dynamics ranging from roots and root hairs, guard cells, pollen and leaves upon mechanical and herbivore damage.	[19,27,61,79,82,84,86–89,92,94,96,98–101]

8. Conclusions and Future Perspectives

Imaging Ca^{2+} in living cells has seen a tremendous development in the last two decades with the evolution of genetically encoded Ca^{2+} indicators. Despite these improvements, we are still far from having an ideal Ca^{2+} probe. Here we give emphasis on future directions on the improvements of synthetic and fluorescent Ca^{2+} probes.

Currently, there are only two ratiometric dyes fura-2 and indo-1 available since thirty years after their synthesis. Both these dyes requires UV spectrum for their excitation. As a result, there is the need for the use of expensive UV lasers for confocal microscopes, with the results of toxicity of UV illumination, lower penetration and background fluorescence. Therefore, it is necessary to develop new indicators that absorb light in the visible range.

The advent of a new generation of protein-based Ca^{2+} indicators has reduced the demand to develop new optimized dyes. Although these protein-based probes offer many advantages over synthetic dyes they are still far from being ideal probes. Most of the GFP-based probes have CaM as Ca^{2+} sensing component. CaMs are also known to be important for many physiological processes in plant system.

Overexpression of GFP-based probes might result in the substantial alteration of endogenous physiological processes that depend on CaM activity [81,102]. Therefore, efforts should focus on designing new protein-based constructs as selective and sensitive as CaM but characterized by a lower or negligible interference with the endogenous components of the plant cell [102]. Further improvements on GFP-based probes should face the problem of bleaching and photoisomerization of GFP upon illumination [103]. Finding novel fluorescent protein from other organisms (other than *Aequorea*) would provide solutions to these problems. All these efforts will allow us to understand the complex subcellular interplay of Ca²⁺ signals underlying many plant physiological and developmental processes.

Acknowledgments

The research leading to the results reported here has received funding from the Autonomous Province of Trento, Italy, with reference to the Call 1-post-doc 2012–Incoming, approved with provincial government resolution No. 1023 of 5/7/10.

Conflicts of Interest

The authors declare no conflict of interest.

References

1. Whalley, H.J.; Knight, M.R. Calcium signatures are decoded by plants to give specific gene responses. *New Phytol.* **2013**, *197*, 690–693.
2. Arimura, G.; Maffei, M.E. Calcium and secondary CPK signaling in plants in response to herbivore attack. *Biochem. Biophys. Res. Commun.* **2010**, *400*, 455–460.
3. McAinsh, M.R.; Pittman, J.K. Shaping the calcium signature. *New Phytol.* **2009**, *181*, 275–294.
4. White, P.J.; Broadley, M.R. Calcium in plants. *Ann. Bot.* **2003**, *92*, 487–511.
5. Monshausen, G.B. Visualizing Ca⁽²⁺⁾ signatures in plants. *Curr. Opin. Plant Biol.* **2012**, *15*, 677–682.
6. Quiles-Pando, C.; Rexach, J.; Navarro-Gochicoa, M.T.; Camacho-Cristobal, J.J.; Herrera-Rodriguez, M.B.; Gonzalez-Fontes, A. Boron deficiency increases the levels of cytosolic Ca⁽²⁺⁾ and expression of Ca⁽²⁺⁾-related genes in *Arabidopsis thaliana* roots. *Plant Physiol. Biochem.* **2013**, *65*, 55–60.
7. Swanson, S.J.; Gilroy, S. Imaging changes in cytoplasmic calcium using the Yellow Cameleon 3.6 biosensor and confocal microscopy. *Methods Mol. Biol.* **2013**, *1009*, 291–302.
8. Choi, W.G.; Swanson, S.J.; Gilroy, S. High-resolution imaging of Ca²⁺, redox status, ROS and pH using GFP biosensors. *Plant J.* **2012**, *70*, 118–128.
9. Batic, O.; Kudla, J. Analysis of calcium signaling pathways in plants. *Biochim. Biophys. Acta* **2012**, *1820*, 1283–1293.
10. Dodd, A.N.; Kudla, J.; Sanders, D. The language of calcium signaling. *Ann. Rev. Plant Biol.* **2010**, *61*, 593–620.

11. McAinsh, M.R.; Ng, C.K. Measurement of cytosolic-free Ca²⁺ in plant tissue. *Methods Mol. Biol.* **2013**, *937*, 327–341.
12. Stael, S.; Wurzinger, B.; Mair, A.; Mehler, N.; Vothknecht, U.C.; Teige, M. Plant organellar calcium signalling: An emerging field. *J. Exp. Bot.* **2012**, *63*, 1525–1542.
13. Behera, S.; Krebs, M.; Loro, G.; Schumacher, K.; Costa, A.; Kudla, J. Ca²⁺ imaging in plants using genetically encoded Yellow Cameleon Ca²⁺ indicators. *Cold Spring Harb. Protoc.* **2013**, *2013*, 700–703.
14. Loro, G.; Ruberti, C.; Zottini, M.; Costa, A. The D3cpv Cameleon reports Ca²⁺ dynamics in plant mitochondria with similar kinetics of the YC3.6 Cameleon, but with a lower sensitivity. *J. Microsc.* **2013**, *249*, 8–12.
15. Bonza, M.C.; Loro, G.; Behera, S.; Wong, A.; Kudla, J.; Costa, A. Analyses of Ca²⁺ accumulation and dynamics in the endoplasmic reticulum of Arabidopsis root cells using a genetically encoded Cameleon sensor. *Plant Physiol.* **2013**, *163*, 1230–1241.
16. Loro, G.; Drago, I.; Pozzan, T.; Schiavo, F.L.; Zottini, M.; Costa, A. Targeting of Cameleons to various subcellular compartments reveals a strict cytoplasmic/mitochondrial Ca²⁺ handling relationship in plant cells. *Plant J.* **2012**, *71*, 1–13.
17. Costa, A.; Drago, I.; Behera, S.; Zottini, M.; Pizzo, P.; Schroeder, J.I.; Pozzan, T.; Lo Schiavo, F. H₂O₂ in plant peroxisomes: An *in vivo* analysis uncovers a Ca²⁺-dependent scavenging system. *Plant J.* **2010**, *62*, 760–772.
18. Logan, D.C.; Knight, M.R. Mitochondrial and cytosolic calcium dynamics are differentially regulated in plants. *Plant Physiol.* **2003**, *133*, 21–24.
19. Iwano, M.; Entani, T.; Shiba, H.; Kakita, M.; Nagai, T.; Mizuno, H.; Miyawaki, A.; Shoji, T.; Kubo, K.; Isogai, A.; *et al.* Fine-tuning of the cytoplasmic Ca²⁺ concentration is essential for pollen tube growth. *Plant Physiol.* **2009**, *150*, 1322–1334.
20. Mithofer, A.; Mazars, C.; Maffei, M.E. Probing Spatio-temporal Intracellular Calcium Variations in Plants. *Methods Mol. Biol.* **2009**, *479*, 79–92.
21. Swanson, S.J.; Choi, W.G.; Chanoca, A.; Gilroy, S. *In vivo* imaging of Ca²⁺, pH, and reactive oxygen species using fluorescent probes in plants. *Ann. Rev. Plant Biol.* **2011**, *62*, 273–297.
22. Joy, M.J.; Pyniarlang, N.; Ralf, O.; Irena, S. Calcium signaling and cytosolic calcium measurements in plants. *J. Endocytobiosis Cell Res.* **2011**, *21*, 64–76.
23. Reddy, G.V.; Gordon, S.P.; Meyerowitz, E.M. Unravelling developmental dynamics: Transient intervention and live imaging in plants. *Nat. Rev. Mol. Cell Biol.* **2007**, *8*, 491–501.
24. Foldes-Papp, Z.; Demel, U.; Tilz, G.P. Laser scanning confocal fluorescence microscopy: An overview. *Int. Immunopharmacol.* **2003**, *3*, 1715–1729.
25. Kohler, B.; Blatt, M.R. Protein phosphorylation activates the guard cell Ca²⁺ channel and is a prerequisite for gating by abscisic acid. *Plant J.* **2002**, *32*, 185–194.
26. Garcia-Mata, C.; Gay, R.; Sokolovski, S.; Hills, A.; Lamattina, L.; Blatt, M.R. Nitric oxide regulates K⁺ and Cl⁻ channels in guard cells through a subset of abscisic acid-evoked signaling pathways. *Proc. Natl. Acad. Sci. USA* **2003**, *100*, 11116–11121.
27. Allen, G.J.; Kwak, J.M.; Chu, S.P.; Llopis, J.; Tsien, R.Y.; Harper, J.F.; Schroeder, J.I. Cameleon calcium indicator reports cytoplasmic calcium dynamics in Arabidopsis guard cells. *Plant J.* **1999**, *19*, 735–747.

28. Costa, A.; Candeo, A.; Fieramonti, L.; Valentini, G.; Bassi, A. Calcium dynamics in root cells of *Arabidopsis thaliana* visualized with selective plane illumination microscopy. *PLoS One* **2013**, *8*, e75646.
29. Tsien, R.Y. New calcium indicators and buffers with high selectivity against magnesium and protons: design, synthesis, and properties of prototype structures. *Biochemistry* **1980**, *19*, 2396–2404.
30. Rudolf, R.; Mongillo, M.; Rizzuto, R.; Pozzan, T. Looking forward to seeing calcium. *Nat. Rev. Mol. Cell Biol.* **2003**, *4*, 579–586.
31. Shimomura, O.; Johnson, F.H.; Saiga, Y. Extraction, purification and properties of aequorin, a bioluminescent protein from the luminous hydromedusan. *Aequorea. J. Cell Comp. Physiol.* **1962**, *59*, 223–239.
32. Knight, M.R.; Read, N.D.; Campbell, A.K.; Trewavas, A.J. Imaging calcium dynamics in living plants using semi-synthetic recombinant aequorins. *J. Cell Biol.* **1993**, *121*, 83–90.
33. Miyawaki, A.; Llopis, J.; Heim, R.; McCaffery, J.M.; Adams, J.A.; Ikura, M.; Tsien, R.Y. Fluorescent indicators for Ca²⁺ based on green fluorescent proteins and calmodulin. *Nature* **1997**, *388*, 882–887.
34. Jares-Erijman, E.A.; Jovin, T.M. FRET imaging. *Nat. Biotechnol.* **2003**, *21*, 1387–1395.
35. Sekar, R.B.; Periasamy, A. Fluorescence resonance energy transfer (FRET) microscopy imaging of live cell protein localizations. *J. Cell Biol.* **2003**, *160*, 629–633.
36. Arimura, G.; Kopke, S.; Kunert, M.; Volpe, V.; David, A.; Brand, P.; Dabrowska, P.; Maffei, M.E.; Boland, W. Effects of feeding *Spodoptera littoralis* on lima bean leaves: IV. Diurnal and nocturnal damage differentially initiate plant volatile emission. *Plant Physiol.* **2008**, *146*, 965–973.
37. Kanchiswamy, C.N.; Mohanta, T.K.; Capuzzo, A.; Occhipinti, A.; Verrillo, F.; Maffei, M.E.; Malnoy, M. Differential expression of CPKs and cytosolic Ca²⁺ variation in resistant and susceptible apple cultivars (*Malus × domestica*) in response to the pathogen *Erwinia amylovora* and mechanical wounding. *BMC Genomics* **2013**, *14*, 760.
38. Kanchiswamy, C.N.; Takahashi, H.; Quadro, S.; Maffei, M.E.; Bossi, S.; Berteau, C.; Zebelo, S.A.; Muroi, A.; Ishihama, N.; Yoshioka, H.; *et al.* Regulation of *Arabidopsis* defense responses against *Spodoptera littoralis* by CPK-mediated calcium signaling. *BMC Plant Biol.* **2010**, *10*, 97.
39. Grynkiewicz, G.; Poenie, M.; Tsien, R.Y. A new generation of Ca²⁺ indicators with greatly improved fluorescence properties. *J. Biol. Chem.* **1985**, *260*, 3440–3450.
40. Pierson, E.S.; Miller, D.D.; Callahan, D.A.; Shipley, A.M.; Rivers, B.A.; Cresti, M.; Hepler, P.K. Pollen tube growth is coupled to the extracellular calcium ion flux and the intracellular calcium gradient: effect of BAPTA-type buffers and hypertonic media. *Plant Cell* **1994**, *6*, 1815–1828.
41. Bothwell, J.H.; Brownlee, C.; Hetherington, A.M.; Ng, C.K.; Wheeler, G.L.; McAinsh, M.R. Biolistic delivery of Ca²⁺ dyes into plant and algal cells. *Plant J.* **2006**, *46*, 327–335.
42. Romano, L.A.; Jacob, T.; Gilroy, S.; Assmann, S.M. Increases in cytosolic Ca²⁺ are not required for abscisic acid-inhibition of inward K⁺ currents in guard cells of *Vicia faba* L. *Planta* **2000**, *211*, 209–217.

43. Zebelo, S.A.; Matsui, K.; Ozawa, R.; Maffei, M.E. Plasma membrane potential depolarization and cytosolic calcium flux are early events involved in tomato (*Solanum lycopersicon*) plant-to-plant communication. *Plant Sci. Biol.* **2012**, *196*, 93–100.
44. Bricchi, I.; Occhipinti, A.; Berteza, C.M.; Zebelo, S.A.; Brillada, C.; Verrillo, F.; de Castro, C.; Molinaro, A.; Faulkner, C.; Maule, A.J.; *et al.* Separation of early and late responses to herbivory in *Arabidopsis* by changing plasmodesmal function. *Plant J.* **2012**, doi:10.1111/j.1365-313X.2012.05103.x.
45. Bush, D.S. Regulation of cytosolic calcium in plants. *Plant Physiol.* **1993**, *103*, 7–13.
46. Dauphin, A.; Gerard, J.; Lapeyrie, F.; Legue, V. Fungal hypaphorine reduces growth and induces cytosolic calcium increase in root hairs of *Eucalyptus globulus*. *Protoplasma* **2007**, *231*, 83–88.
47. Zhang, W-H.; Rengel, Z.; Kuo, J. Determination of intracellular Ca²⁺ in cells of intact wheat roots: Loading of acetoxymethyl ester of Fluo-3 under low temperature. *Plant J.* **1998**, *15*, 147–151.
48. Bush, D.S.; Biswas, A.K.; Jones, R.L. Gibberellic-acid-stimulated Ca²⁺ accumulation in endoplasmic reticulum of barley aleurone: Ca²⁺ transport and steady-state levels. *Planta* **1989**, *178*, 411–420.
49. Maffei, M.; Bossi, S.; Spiteller, D.; Mithofer, A.; Boland, W. Effects of feeding *Spodoptera littoralis* on lima bean leaves. I. Membrane potentials, intracellular calcium variations, oral secretions, and regurgitate components. *Plant Physiol.* **2004**, *134*, 1752–1762.
50. Mohanta, T.K.; Occhipinti, A.; Zebelo, S.A.; Foti, M.; Fliegmann, J.; Bossi, S.; Maffei, M.E.; Berteza, C.M. *Ginkgo biloba* responds to herbivory by activating early signaling and direct defenses. *PLoS One* **2012**, *7*, e32822.
51. Qu, H.; Jiang, X.; Shi, Z.; Liu, L.; Zhang, S. Fast loading ester fluorescent Ca²⁺ and pH indicators into pollen of *Pyrus pyrifolia*. *J. Plant Res.* **2012**, *125*, 185–195.
52. Zhao, X.; Wang, Y.J.; Wang, Y.L.; Wang, X.L.; Zhang, X. Extracellular Ca²⁺ alleviates NaCl-induced stomatal opening through a pathway involving H₂O₂-blocked Na⁺ influx in *Vicia* guard cells. *J. Plant Physiol.* **2011**, *168*, 903–910.
53. Liu, G.; Dang, L.; Wang, D.M. The influence of elicitor on the distribution pattern of microtubule and the cytosolic calcium in mesophyll protoplast of wheat. *Fen Zi Xi Bao Sheng Wu Xue Bao* **2007**, *40*, 205–213.
54. Nair, R.; Raina, S.; Keshavarz, T.; Kerrigan, M.J. Application of fluorescent indicators to analyse intracellular calcium and morphology in filamentous fungi. *Fungal Biol.* **2011**, *115*, 326–334.
55. Schulz, A.; Woolley, R.; Tabarin, T.; McDonagh, C. Dextran-coated silica nanoparticles for calcium-sensing. *Analyst* **2011**, *136*, 1722–1727.
56. Wu, X.; Chen, T.; Zheng, M.; Chen, Y.; Teng, N.; Samaj, J.; Baluska, F.; Lin, J. Integrative proteomic and cytological analysis of the effects of extracellular Ca²⁺ influx on *Pinus bungeana* pollen tube development. *J. Proteome Res.* **2008**, *7*, 4299–4312.
57. Lu, Y.; Paige, M.F. An ensemble and single-molecule fluorescence spectroscopy investigation of Calcium Green 1, a calcium-ion sensor. *J. Fluoresc.* **2007**, *17*, 739–748.
58. Bagh, S.; Paige, M.F. Ensemble and single-molecule fluorescence spectroscopy of a calcium-ion indicator dye. *J. Phys. Chem. A* **2006**, *110*, 7057–7066.

59. Braun, M.; Richter, P. Relocalization of the calcium gradient and a dihydropyridine receptor is involved in upward bending by bulging of *Chara* protonemata, but not in downward bending by bowing of *Chara* rhizoids. *Planta* **1999**, *209*, 414–423.
60. Bunney, T.D.; Shaw, P.J.; Watkins, P.A.; Taylor, J.P.; Beven, A.F.; Wells, B.; Calder, G.M.; Drobak, B.K. ATP-dependent regulation of nuclear Ca^{2+} levels in plant cells. *FEBS Lett.* **2000**, *476*, 145–149.
61. Baird, G.S.; Zacharias, D.A.; Tsien, R.Y. Circular permutation and receptor insertion within green fluorescent proteins. *Proc. Natl. Acad. Sci. USA* **1999**, *96*, 11241–11246.
62. Ottolini, D.; Cali, T.; Brini, M. Measurements of Ca^{2+} concentration with recombinant targeted luminescent probes. *Methods Mol. Biol.* **2013**, *937*, 273–291.
63. Zhu, X.; Feng, Y.; Liang, G.; Liu, N.; Zhu, J.K. Aequorin-based luminescence imaging reveals stimulus- and tissue-specific Ca^{2+} dynamics in *Arabidopsis* plants. *Mol. Plant* **2013**, *6*, 444–455.
64. Knight, H.; Knight, M.R. Recombinant aequorin methods for intracellular calcium measurement in plants. *Methods Cell Biol.* **1995**, *49*, 201–216.
65. Brini, M.; Cali, T.; Ottolini, D.; Carafoli, E. Intracellular calcium homeostasis and signaling. *Met. Ions Life Sci.* **2013**, *12*, 119–168.
66. Cali, T.; Ottolini, D.; Brini, M. Calcium and endoplasmic reticulum-mitochondria tethering in neurodegeneration. *DNA Cell Biol.* **2013**, *32*, 140–146.
67. Bonora, M.; Giorgi, C.; Bononi, A.; Marchi, S.; Patergnani, S.; Rimessi, A.; Rizzuto, R.; Pinton, P. Subcellular calcium measurements in mammalian cells using jellyfish photoprotein aequorin-based probes. *Nat. Protoc.* **2013**, *8*, 2105–2118.
68. Pozzan, T.; Rizzuto, R. Imaging calcium dynamics using targeted recombinant aequorins. *CSH Protoc.* **2008**, *2008*, doi:10.1101/pdb.top26.
69. Rizzuto, R.; Pinton, P.; Brini, M.; Chiesa, A.; Filippin, L.; Pozzan, T. Mitochondria as biosensors of calcium microdomains. *Cell Calcium* **1999**, *26*, 193–199.
70. Brini, M.; Pinton, P.; Pozzan, T.; Rizzuto, R. Targeted recombinant aequorins: Tools for monitoring $[\text{Ca}^{2+}]$ in the various compartments of a living cell. *Microsc. Res. Tech.* **1999**, *46*, 380–389.
71. Pinton, P.; Brini, M.; Bastianutto, C.; Tuft, R.A.; Pozzan, T.; Rizzuto, R. New light on mitochondrial calcium. *BioFactors* **1998**, *8*, 243–253.
72. Pinton, P.; Pozzan, T.; Rizzuto, R. The Golgi apparatus is an inositol 1,4,5-trisphosphate-sensitive Ca^{2+} store, with functional properties distinct from those of the endoplasmic reticulum. *EMBO J.* **1998**, *17*, 5298–5308.
73. Maffei, M.E.; Mithofer, A.; Arimura, G.; Uchtenhagen, H.; Bossi, S.; Berteza, C.M.; Cucuzza, L.S.; Novero, M.; Volpe, V.; Quadro, S.; *et al.* Effects of feeding *Spodoptera littoralis* on lima bean leaves. III. Membrane depolarization and involvement of hydrogen peroxide. *Plant Physiol.* **2006**, *140*, 1022–1035.
74. Marti, M.C.; Stancombe, M.A.; Webb, A.A. Cell- and stimulus type-specific intracellular free Ca^{2+} signals in *Arabidopsis*. *Plant Physiol.* **2013**, *163*, 625–634.
75. Allen, D.G.; Blinks, J.R.; Prendergast, F.G. Aequorin luminescence: Relation of light emission to calcium concentration—A calcium-independent component. *Science* **1977**, *195*, 996–998.

76. Romoser, V.A.; Hinkle, P.M.; Persechini, A. Detection in living cells of Ca²⁺-dependent changes in the fluorescence emission of an indicator composed of two green fluorescent protein variants linked by a calmodulin-binding sequence. A new class of fluorescent indicators. *J. Biol. Chem.* **1997**, *272*, 13270–13274.
77. Whitaker, M. Genetically encoded probes for measurement of intracellular calcium. *Methods Cell Biol.* **2010**, *99*, 153–182.
78. Tozawa, Y.; Nozawa, A.; Kanno, T.; Narisawa, T.; Masuda, S.; Kasai, K.; Nanamiya, H. Calcium-activated (p)ppGpp synthetase in chloroplasts of land plants. *J. Biol. Chem.* **2007**, *282*, 35536–35545.
79. Nagai, T.; Sawano, A.; Park, E.S.; Miyawaki, A. Circularly permuted green fluorescent proteins engineered to sense Ca²⁺. *Proc. Natl. Acad. Sci. USA* **2001**, *98*, 3197–3202.
80. Miyawaki, A.; Griesbeck, O.; Heim, R.; Tsien, R.Y. Dynamic and quantitative Ca²⁺ measurements using improved cameleons. *Proc. Natl. Acad. Sci. USA* **1999**, *96*, 2135–2140.
81. Palmer, A.E.; Tsien, R.Y. Measuring calcium signaling using genetically targetable fluorescent indicators. *Nat. Protoc.* **2006**, *1*, 1057–1065.
82. Allen, G.J.; Chu, S.P.; Harrington, C.L.; Schumacher, K.; Hoffmann, T.; Tang, Y.Y.; Grill, E.; Schroeder, J.I. A defined range of guard cell calcium oscillation parameters encodes stomatal movements. *Nature* **2001**, *411*, 1053–1057.
83. Sun, J.; Miwa, H.; Downie, J.A.; Oldroyd, G.E. Mastoparan activates calcium spiking analogous to Nod factor-induced responses in *Medicago truncatula* root hair cells. *Plant Physiol.* **2007**, *144*, 695–702.
84. Miwa, H.; Sun, J.; Oldroyd, G.E.; Downie, J.A. Analysis of Nod-factor-induced calcium signaling in root hairs of symbiotically defective mutants of *Lotus japonicus*. *Mol. Plant-Microbe Interact.* **2006**, *19*, 914–923.
85. Kosuta, S.; Hazledine, S.; Sun, J.; Miwa, H.; Morris, R.J.; Downie, J.A.; Oldroyd, G.E. Differential and chaotic calcium signatures in the symbiosis signaling pathway of legumes. *Proc. Natl. Acad. Sci. USA* **2008**, *105*, 9823–9828.
86. Nagai, T.; Yamada, S.; Tominaga, T.; Ichikawa, M.; Miyawaki, A. Expanded dynamic range of fluorescent indicators for Ca²⁺ by circularly permuted yellow fluorescent proteins. *Proc. Natl. Acad. Sci. USA* **2004**, *101*, 10554–10559.
87. Monshausen, G.B.; Bibikova, T.N.; Messerli, M.A.; Shi, C.; Gilroy, S. Oscillations in extracellular pH and reactive oxygen species modulate tip growth of *Arabidopsis* root hairs. *Proc. Natl. Acad. Sci. USA* **2007**, *104*, 20996–21001.
88. Monshausen, G.B.; Messerli, M.A.; Gilroy, S. Imaging of the Yellow Cameleon 3.6 indicator reveals that elevations in cytosolic Ca²⁺ follow oscillating increases in growth in root hairs of *Arabidopsis*. *Plant Physiol.* **2008**, *147*, 1690–1698.
89. Verrillo, F.; Occhipinti, A.; Kanchiswamy, C.N.; Maffei, M.E. Quantitative analysis of herbivore-induced cytosolic calcium by using a Cameleon (YC 3.6) calcium sensor in *Arabidopsis thaliana*. *J. Plant Physiol.* **2014**, *171*, 136–139.
90. Behera, S.; Kudla, J. High-resolution imaging of cytoplasmic Ca²⁺ dynamics in *Arabidopsis* roots. *Cold Spring Harb. Protoc.* **2013**, *2013*, doi:10.1101/pdb.prot073023.

91. Behera, S.; Kudla, J. Live cell imaging of cytoplasmic Ca²⁺ dynamics in *Arabidopsis* guard cells. *Cold Spring Harb. Protoc.* **2013**, *2013*, 665–669.
92. Monshausen, G.B.; Bibikova, T.N.; Weisenseel, M.H.; Gilroy, S. Ca²⁺ regulates reactive oxygen species production and pH during mechanosensing in *Arabidopsis* roots. *Plant Cell* **2009**, *21*, 2341–2356.
93. Gjetting, S.K.; Schulz, A.; Fuglsang, A.T. Perspectives for using genetically encoded fluorescent biosensors in plants. *Front. Plant Sci.* **2013**, *4*, 234.
94. Allen, G.J.; Murata, Y.; Chu, S.P.; Nafisi, M.; Schroeder, J.I. Hypersensitivity of abscisic acid-induced cytosolic calcium increases in the *Arabidopsis* farnesyltransferase mutant *eral-2*. *Plant Cell* **2002**, *14*, 1649–1662.
95. Allen, G.J.; Chu, S.P.; Schumacher, K.; Shimazaki, C.T.; Vafeados, D.; Kemper, A.; Hawke, S.D.; Tallman, G.; Tsien, R.Y.; Harper, J.F.; *et al.* Alteration of stimulus-specific guard cell calcium oscillations and stomatal closing in *Arabidopsis det3* mutant. *Science* **2000**, *289*, 2338–2342.
96. Allen, G.J.; Kuchitsu, K.; Chu, S.P.; Murata, Y.; Schroeder, J.I. *Arabidopsis abi1-1* and *abi2-1* phosphatase mutations reduce abscisic acid-induced cytoplasmic calcium rises in guard cells. *Plant Cell* **1999**, *11*, 1785–1798.
97. Sieberer, B.J.; Chabaud, M.; Timmers, A.C.; Monin, A.; Fournier, J.; Barker, D.G. A nuclear-targeted cameleon demonstrates intranuclear Ca²⁺ spiking in *Medicago truncatula* root hairs in response to rhizobial nodulation factors. *Plant Physiol.* **2009**, *151*, 1197–1206.
98. Iwano, M.; Shiba, H.; Miwa, T.; Che, F.S.; Takayama, S.; Nagai, T.; Miyawaki, A.; Isogai, A. Ca²⁺ dynamics in a pollen grain and papilla cell during pollination of *Arabidopsis*. *Plant Physiol.* **2004**, *136*, 3562–3571.
99. Miwa, H.; Sun, J.; Oldroyd, G.E.; Downie, J.A. Analysis of calcium spiking using a cameleon calcium sensor reveals that nodulation gene expression is regulated by calcium spike number and the developmental status of the cell. *Plant J.* **2006**, *48*, 883–894.
100. Richter, G.L.; Monshausen, G.B.; Krol, A.; Gilroy, S. Mechanical stimuli modulate lateral root organogenesis. *Plant Physiol.* **2009**, *151*, 1855–1866.
101. Rincon-Zachary, M.; Teaster, N.D.; Sparks, J.A.; Valster, A.H.; Motes, C.M.; Blancaflor, E.B. Fluorescence resonance energy transfer-sensitized emission of yellow cameleon 3.60 reveals root zone-specific calcium signatures in *Arabidopsis* in response to aluminum and other trivalent cations. *Plant Physiol.* **2010**, *152*, 1442–1458.
102. Palmer, A.E.; Giacomello, M.; Kortemme, T.; Hires, S.A.; Lev-Ram, V.; Baker, D.; Tsien, R.Y. Ca²⁺ indicators based on computationally redesigned calmodulin-peptide pairs. *Chem. Biol.* **2006**, *13*, 521–530.
103. Patterson, G.H.; Knobel, S.M.; Sharif, W.D.; Kain, S.R.; Piston, D.W. Use of the green fluorescent protein and its mutants in quantitative fluorescence microscopy. *Biophys. J.* **1997**, *73*, 2782–2790.